Design and Optimization of a 6-DOF Singularity-Free Parallel Manipulator

Guotao Li, Hailin Huang and Bing Li*

Shenzhen Graduate School, Harbin Institute of Technology, China

Abstract: A novel six degrees-of-freedom (DOF) singularity-free parallel manipulator (PM) is presented. The PM consists of five peripheral limbs and a centre limb, which makes the mechanism have high stiffness and large tilting capability . Due to the special architecture, the doubly actuated centre limb of the manipulator could have infinite inverse solutions. In every configuration of the end-effector, the manipulator can adapt its centre limb to the position and orientation with best dexterities. Targeting for further analysis of the manipulator, its detailed kinematic analysis is developed, including the solutions of the inverse position problems, the singularity, the dexterity and the workspace. The analysis results show that the proposed manipulator has good performance and thus may be suitable candidate for complicated surface machining.

Keywords: Parallel manipulator, Singularity-free Workspace.

1. INTRODUCTION

Parallel mechanism has been widely applied in the modern manufacturing industry due to the many advantages such as high stiffness, large load capacity, high precision potential and good dynamic performance, etc that are profit from the multiple closed-loop structure between the fixed platform and the moving platform [1]. In addition to 6-DOF Stewart platform [2], the parallel mechanisms of Tricept robot [3] and Delta robot [4] have been popularly used in modern industries. In the kinematic analysis of parallel mechanism, the key to the forward kinematic solution is to solve the higher-order nonlinear constraint equations, which is very complex, while the inverse problem is mainly to solve the input of the problem according to the position and orientation of the end-effector of the parallel mechanism. The numerical method [5,6] and the analytical approach [7,9] are two main methods in the positional analysis of the parallel mechanism. Stock and Miller [10] combined the manipulability and the workspace as the objective, where the weighting factors are used to evaluate the relative importance between the two performances, so a multi-objective optimization problem is addressed.

In recent years, many effective design approaches have been adopted to improve the PMs' manufacturing capacities, such as workspace size, tilting capacity, systematic stiffness, etc [1].

In this paper, a novel 6-DOF singularity-free parallel manipulator is introduced. The proposed parallel manipulator consists of five peripheral limbs with two different configurations, and one centre limb with two driving pairs. Due to the special architecture, the doubly actuated centre limb of the parallel manipulator has infinite inverse solutions for a given configuration of the end-effector. This makes the manipulator capable of achieving continuous singularity-free motion path. The design and optimization of the proposed parallel manipulator are investigated in details.

The paper is organized as follows. In section 2 a novel parallel manipulator with an adaptable central chain is proposed, and the kinematic analysis of the parallel manipulator, including the inverse position problem and Jacobian matrix problem between the input and the output, is presented. The dexterity is introduced for the parallel manipulator singularity analysis, and the workspace is obtained by the dexterity index in Section 3. The conclusions are given in Section 4.

2. MECHANISM SCHEME AND INVERSE KINEMATICS

2.1. Mechanism Scheme

As shown in Figure **1**, the scheme of the parallel manipulator proposed in this paper is composed of three peripheral PUS (Prismatic-Universal-Spherical joints) limbs, two SPU (Spherical-Prismatic-T Universal joints) limbs and one PPUU (Prismatic-Prismatic-Universal-Universal joints) centre limb. The three peripheral PUS limbs and two SPU limbs are actuated by the five prismatic joints P_i, i=1,2,3,4,5 and the PPUU centre limb is actuated by two prismatic joints P_6 and P_7. The notations given in Figure **2** are as follows: each PUS and SPU limb i consists of one actuated prismatic

*Address correspondence to this author at the Shenzhen Graduate School, Harbin Institute of Technology China; Tel: 0755-26033485;
Fax: 0755-26033485; E-mail: libing.sgs@hit.edu.cn

E-ISSN: 2409-9694/14

joint P_i, one universal joint U_i and other three revolute joints whose joint axes are concurrent at a point N_i. U_6 and N_6 are the two universal joints of the centre limb; P_i, i=1,2,3,…,7 are the seven actuated prismatic joints of the manipulator; O-xyz is the fixed coordinate system with the X-axis directing to the point A_1, and the origin O of the fixed coordinate is the centre of the pentagon; $N_1N_2N_3N_4N_5$ is designed with the pentagon shape and the moving coordinate system attached to the moving platform is located at the centre of the pentagon with x-axis pointing to N_1. All the five actuated prismatic joints for PUS and SPU limbs can travel along the corresponding direction and the two actuated prismatic joints P_6 and P_7 for the PPUU centre limb can travel along the x and y directions respectively.

Figure 1: Proposed parallel mechanism.

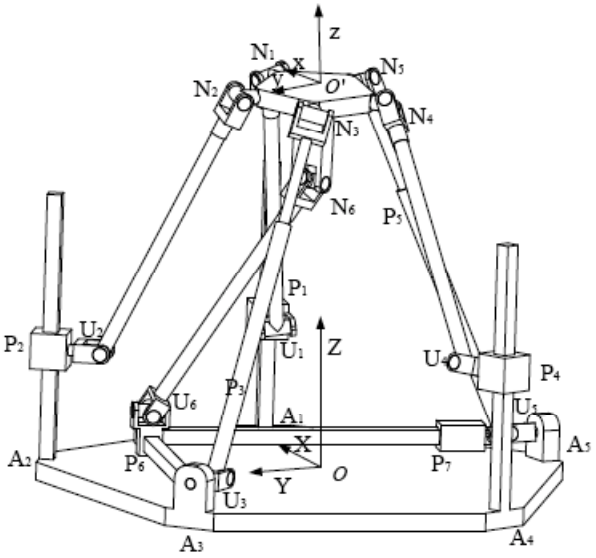

Figure 2: Coordinate frames of the mechanism.

2.2. Position Analysis

The dimensional parameters of this manipulator are given as follows: $OA_i = R, O'N_i = r, U_1N_1 = U_2N_2 = U_4N_4 = a, O'N_i = r$, $O'N_6 = b, U_6N_6 = c$. When the manipulator is at its home configuration, the z'-axis of the moving coordinate coincides with z-axis of the fixed coordinate and the x', y' directions are parallel to the x, y directions, respectively.

$(x, y, z, \phi, \theta, \psi)$ is used to describe the position and orientation of the moving platform with respect to the fixed coordinate frame O-xyz, where the triple elements (x,y,z) represents the position coordinate of the moving platform and the other three elements (ϕ, θ, ψ) represents the tiling and the torsion angles of the moving platform. One choose XYZ fixed angles to represent the orientation matrix R describing the orientation of the moving coordinate frame to the fixed coordinate frame. The resulting rotation matrix in terms of these angle coordinates can be given by

$$[\boldsymbol{R}] = [{}^{\phi}\boldsymbol{R}_z][{}^{\theta}\boldsymbol{R}_y][{}^{\psi}\boldsymbol{R}] = \begin{pmatrix} C_\phi C_\theta C_\psi - S_\phi S_\psi & -C_\phi C_\theta C_\psi - S_\phi C_\psi & C_\phi S_\theta \\ S_\phi C_\theta C_\psi + C_\phi C_\psi & -S_\phi C_\theta S_\psi + C_\phi C_\psi & S_\phi S_\theta \\ -S_\theta S_\psi & S_\theta S_\psi & C_\theta \end{pmatrix} \quad (1)$$

where S denotes the sinusoidal function and C denotes the cosine function. Then the six pivots $N_1, N_2, N_3, N_4, N_5, N_6$ can be expressed as the vector $\overrightarrow{ON_i}$:

$$\overrightarrow{\mathbf{ON}_i} = [\mathbf{R}]\overrightarrow{\mathbf{O'N}_i} + \overrightarrow{\mathbf{OO'}}, \ i=1,2,3,4,5,6. \quad (2)$$

The representations of the key points attached to the moving and fixed coordinate system can be expressed as follows:

$$\overrightarrow{\mathbf{O'N}_i} = \left(r\cos\frac{2(i-1)\pi}{5}, r\sin\frac{2(i-1)\pi}{5}, 0 \right) \quad (3)$$

$$\overrightarrow{\mathbf{OA}_i} = \left(R\cos\frac{2(i-1)\pi}{5}, R\sin\frac{2(i-1)\pi}{5}, 0 \right) \quad (4)$$

in which *i*=1,2,3,4,5.

2.3. Inverse kinematics

The inverse displacement solution is to obtain the input position of the driving pairs for the given positions and orientations of the moving platform [11]. To obtain the input position, One can use the geometric const-raint equation to obtain the respective loop closure equation, and then get the corresponding solution.

As for the PUS chains, using the geometric constraint equations

$$\left\|\overrightarrow{\mathbf{U}_i\mathbf{N}_i}\right\| = c, (i = 1,2,4) \tag{5}$$

we can easily get the lengths of $L_i\,(i = 1,2,4)$:

$$L_i = Z_{N_i} - \sqrt{a^2 - \left(X_{N_i} - X_{A_i}\right)^2 - \left(Y_{N_i} - Y_{A_i}\right)^2} \tag{6}$$

where X_{N_i} is the first, Y_{N_i} is the second, Z_{N_i} is the third element of the vector $\overrightarrow{\mathbf{O'N}_i}$.

With respect to the SPU chain, the following geometric constraint equations can be obtained as follows:

$$\overrightarrow{\mathbf{A}_i\mathbf{N}_i} = L_i\vec{\mathbf{u}} = \left(X_{N_i} - X_{A_i} \quad Y_{N_i} - Y_{A_i} \quad Z_{N_i}\right)(i = 3,5) \tag{7}$$

Take the F-norm of Eq.(2), then we can obtain

$$\begin{cases} L_i = \sqrt{\left(X_{N_i} - X_{A_i}\right)^2 + \left(Y_{N_i} - Y_{A_i}\right)^2 + {Z_{N_i}}^2} \\ \vec{\mathbf{u}}_i = \left(\dfrac{X_{N_i} - X_{A_i}}{L_i} \quad \dfrac{Y_{N_i} - Y_{A_i}}{L_i} \quad \dfrac{Z_{N_i}}{L_i}\right) \end{cases} \tag{8}$$

Where X_{A_i} is the first, Y_{A_i} is the second element of the vector $\overrightarrow{\mathbf{OA}_i}$.

With respect to the central chain PPUS, similarly we can have the following geometric constraints equation:

$$\left\|\overrightarrow{\mathbf{U}_6\mathbf{N}_6}\right\| = c \tag{9}$$

which can be expanded into

$$\left(X_{N_6} - L_6\right)^2 + \left(Y_{N_6} - L_7\right)^2 + \left(Z_{N_6} - 0\right)^2 = c^2 \tag{10}$$

where L_6 and L_7 is the displacement of the two actuated prismatic joints P_6 and P_7 for the PPUU centre limb.

Eq.(6), Eq.(8) and Eq.(10) can be combined into the total geometric constraint equations, which is a 6 scalar equation array with 13 variables, i.e. the 7 actuated joint variables L_i, i=1,2,…,7, and the 6 pose coordinates $(x, y, z, \phi, \theta, \psi)$.so the position problems have infinite solutions.

For the centre limb, we have the relation in Eq.(10), which represents that for a given pose $(x, y, z, \phi, \theta, \psi)$ of the end-effector the actuated prismatic joints P_6 and P_7 can be free to move in the circle M centring in $\left(X_{N_6}, Y_{N_6}, Z_{N_6}\right)$ with the radius of $\sqrt{c^2 - \left(0 - Z_{N_6}\right)^2}$. The inverse kinematic problem for such a centre limb is ill-posed because there may exist infinite possible configurations of the manipulator which determine the same end-effector pose. Additional criteria are used to determine the proper inverse solution of the centre limb in this paper. In order to improve the performance index of the manipulator, one can introduce an optimization constraint to come it true. Assuming that the end-effector is at the current pose $X = (x, y, z, \phi, \theta, \psi)$, we will introduce the optimization constraint as follows:

$$\max\ o(J)$$

$$\text{subject to } \left(X_{N_6} - L_6\right)^2 + \left(Y_{N_6} - L_7\right)^2 + \left(Z_{N_6} - 0\right)^2 = c^2 \tag{11}$$

where $o(J)$ is the performance index related to the Eq.(10). We can choose the dexterity, stiffness, tilting angle, output force, etc. as the index in order to improve the performance in the following terms, such as singularity avoidance, stiffness improvement and tiling capacity improvement, etc.

2.4. Jacobian Matrix

With regard to the PUS chain, we can obtain the following loop vector equations based on the geometry of the manipulator.

$$\overrightarrow{\mathbf{ON}_i} = \overrightarrow{\mathbf{OA}_i} + \overrightarrow{\mathbf{A}_i\mathbf{U}_i} + \overrightarrow{\mathbf{U}_i\mathbf{N}_i}, i = 1,2,4 \tag{12}$$

By differentiating the above Eq.(12) with respect to time, the following expression can be obtained,

$$\vec{\omega} \times \overrightarrow{\mathbf{ON}_i} + \vec{\mathbf{v}} = \dot{\boldsymbol{\theta}}_i + \vec{\omega}_{\overrightarrow{\mathbf{U}_i\mathbf{N}_i}} \times \overrightarrow{\mathbf{U}_i\mathbf{N}_i} \tag{13}$$

Where $\vec{\mathbf{v}}$ is the linear velocity vector of the end-effector; $\vec{\boldsymbol{\omega}}$ is the angular velocity vector of the end-effector; $\vec{\boldsymbol{\omega}}_{\overrightarrow{\mathbf{U}_i\mathbf{N}_i}}$ represents the angular velocity vector along the $\overrightarrow{\mathbf{U}_i\mathbf{N}_i}$ direction. All these description is with respect to the fixed coordinate system. $\dot{\boldsymbol{\theta}}_i = \left(0, 0, \dot{L}_i\right)^T, i = 1,2,4$ is the actuation vector of the limb i.

Taking dot product $\overrightarrow{\mathbf{U}_i\mathbf{N}_i}$ to Eq.(13), it will yield

$$\left(\vec{\boldsymbol{\omega}} \times \overrightarrow{\mathbf{ON}_i} + \vec{\mathbf{v}}\right) \cdot \overrightarrow{\mathbf{U}_i\mathbf{N}_i} = \dot{\boldsymbol{\theta}}_i \cdot \overrightarrow{\mathbf{U}_i\mathbf{N}_i} = \dot{L}_i(Z_{N_i} - L_i) \tag{14}$$

The matrix form of Eq.(14) can be written as (15)

$$\begin{bmatrix} \left(\overrightarrow{\mathbf{U}_1\mathbf{N}_1}\right)^T & \left(\overrightarrow{\mathbf{ON}_1}\times\overrightarrow{\mathbf{U}_1\mathbf{N}_1}\right)^T \\ \left(\overrightarrow{\mathbf{U}_2\mathbf{N}_2}\right)^T & \left(\overrightarrow{\mathbf{ON}_2}\times\overrightarrow{\mathbf{U}_2\mathbf{N}_2}\right)^T \\ \left(\overrightarrow{\mathbf{U}_4\mathbf{N}_4}\right)^T & \left(\overrightarrow{\mathbf{ON}_4}\times\overrightarrow{\mathbf{U}_4\mathbf{N}_4}\right)^T \end{bmatrix} \begin{bmatrix} \vec{\mathbf{v}} \\ \vec{\boldsymbol{\omega}} \end{bmatrix} = \begin{bmatrix} Z_{N_1}-L_1 & 0 & 0 \\ 0 & Z_{N_2}-L_2 & 0 \\ 0 & 0 & Z_{N_4}-L_4 \end{bmatrix} \begin{bmatrix} \dot{L}_1 \\ \dot{L}_2 \\ \dot{L}_4 \end{bmatrix} \quad (15)$$

With regard to the SPU chain, we can obtain the following loop vector equations:

$$\overrightarrow{\mathbf{ON}_i} = \overrightarrow{\mathbf{OU}_i} + \overrightarrow{\mathbf{U}_i\mathbf{N}_i} \quad (16)$$

Differentiating Eq.(16) with respect to time yields

$$\vec{\boldsymbol{\omega}}\times\overrightarrow{\mathbf{ON}_i} + \vec{\mathbf{v}} = \dot{L}_i\vec{\mathbf{u}}_i + L_i(\vec{\boldsymbol{\omega}}\times\vec{\mathbf{u}}_i) \quad (17)$$

Taking dot product $\vec{\mathbf{u}}_i = \dfrac{\overrightarrow{\mathbf{U}_i\mathbf{N}_i}}{L_i}$ to Eq.(17), it yields

$$(\vec{\boldsymbol{\omega}}\times\overrightarrow{\mathbf{ON}_i} + \vec{\mathbf{v}})\cdot\vec{\mathbf{u}}_i = \dot{\mathbf{L}}_i \quad (18)$$

The matrix form of Eq.(18) can be written as follows:

$$\begin{bmatrix} \dot{\mathbf{L}}_3 \\ \dot{\mathbf{L}}_5 \end{bmatrix} = \begin{bmatrix} \vec{\mathbf{u}}_3^{\,T} & \left(\overrightarrow{\mathbf{ON}_3}\times\vec{\mathbf{u}}_3\right)^T \\ \vec{\mathbf{u}}_5^{\,T} & \left(\overrightarrow{\mathbf{ON}_5}\times\vec{\mathbf{u}}_5\right)^T \end{bmatrix} \begin{bmatrix} \vec{\mathbf{v}} \\ \vec{\omega} \end{bmatrix} \quad (19)$$

Note that $\vec{\mathbf{u}}_i = \dfrac{\overrightarrow{\mathbf{U}_i\mathbf{N}_i}}{L_i}$, we can obtain

$$\begin{bmatrix} \overrightarrow{\mathbf{U}_3\mathbf{N}_3}^T & \left(\overrightarrow{\mathbf{ON}_3}\times\overrightarrow{\mathbf{U}_3\mathbf{N}_3}\right)^T \\ \overrightarrow{\mathbf{U}_5\mathbf{N}_5}^T & \left(\overrightarrow{\mathbf{ON}_5}\times\overrightarrow{\mathbf{U}_5\mathbf{N}_5}\right)^T \end{bmatrix} \begin{bmatrix} \vec{\mathbf{v}} \\ \vec{\omega} \end{bmatrix} = \begin{bmatrix} L_3 & 0 \\ 0 & L_5 \end{bmatrix} \begin{bmatrix} \dot{\mathbf{L}}_3 \\ \dot{\mathbf{L}}_5 \end{bmatrix} \quad (20)$$

With regard to the central PPUS chain, we can get the following loop vector equations:

$$\overrightarrow{\mathbf{ON}_6} = \overrightarrow{\mathbf{OU}_6} + \overrightarrow{\mathbf{U}_6\mathbf{N}_6} \quad (21)$$

Differentiating Eq.(21) respect to time yields

$$\vec{\boldsymbol{\omega}}\times\overrightarrow{\mathbf{ON}_6} + \vec{\mathbf{v}} = \dot{\mathbf{U}} + \vec{\boldsymbol{\omega}}\times\overrightarrow{\mathbf{U}_6\mathbf{N}_6} \quad (22)$$

where $\dot{\mathbf{U}} = (L_6 \quad L_7 \quad 0)$.

Multiply $\overrightarrow{\mathbf{U}_i\mathbf{N}_i}$ to Eq.(22), it can be expressed as follows:

$$\left(\vec{\boldsymbol{\omega}}\times\overrightarrow{\mathbf{ON}_6} + \vec{\mathbf{v}}\right)\cdot\overrightarrow{\mathbf{U}_6\mathbf{N}_6} = \dot{\mathbf{U}}^T\cdot\overrightarrow{\mathbf{U}_6\mathbf{N}_6} \quad (23)$$

Eq.(23) can be rewritten as follows:

$$\left[\overrightarrow{\mathbf{U}_6\mathbf{N}_6}^T \quad (\overrightarrow{\mathbf{ON}_6}\times\overrightarrow{\mathbf{U}_6\mathbf{N}_6})^T\right]\begin{bmatrix} \vec{\mathbf{v}} \\ \vec{\omega} \end{bmatrix} = \overrightarrow{\mathbf{U}_6\mathbf{N}_6}^{\mathrm{T}}\cdot\dot{\mathbf{U}} \quad (24)$$

Due to $\overrightarrow{\mathbf{U}_6\mathbf{N}_6}^{\mathrm{T}}\cdot\dot{\mathbf{U}} = \dot{\mathbf{L}}_6(X_{N6}-L_6) + \dot{\mathbf{L}}_7(Y_{N6}-L_7)$, by integrating the respective velocity equations of the three chains above in matrix form, one can obtain the following equation, which can be abbreviated to $J_a\dot{V} = J_\theta\dot{\theta}$.

$$\begin{bmatrix} \overrightarrow{\mathbf{U}_1\mathbf{N}_1}^T & \left(\overrightarrow{\mathbf{ON}_1}\times\overrightarrow{\mathbf{U}_1\mathbf{N}_1}\right)^T \\ \overrightarrow{\mathbf{U}_2\mathbf{N}_2}^T & \left(\overrightarrow{\mathbf{ON}_2}\times\overrightarrow{\mathbf{U}_2\mathbf{N}_2}\right)^T \\ \overrightarrow{\mathbf{U}_3\mathbf{N}_3}^T & \left(\overrightarrow{\mathbf{ON}_3}\times\overrightarrow{\mathbf{U}_3\mathbf{N}_3}\right)^T \\ \overrightarrow{\mathbf{U}_4\mathbf{N}_4}^T & \left(\overrightarrow{\mathbf{ON}_4}\times\overrightarrow{\mathbf{U}_4\mathbf{N}_4}\right)^T \\ \overrightarrow{\mathbf{U}_5\mathbf{N}_5}^T & \left(\overrightarrow{\mathbf{ON}_5}\times\overrightarrow{\mathbf{U}_5\mathbf{N}_5}\right)^T \\ \overrightarrow{\mathbf{U}_6\mathbf{N}_6}^T & \left(\overrightarrow{\mathbf{OU}_6}\times\overrightarrow{\mathbf{U}_6\mathbf{N}_6}\right)^T \end{bmatrix} \begin{bmatrix} \vec{\mathbf{v}} \\ \vec{\boldsymbol{\omega}} \end{bmatrix} = \quad (25)$$

$$\begin{bmatrix} Z_{N_1}-L_1 & 0 & 0 & 0 & 0 & 0 & 0 \\ 0 & Z_{N_2}-L_2 & 0 & 0 & 0 & 0 & 0 \\ 0 & 0 & L_3 & 0 & 0 & 0 & 0 \\ 0 & 0 & 0 & Z_{N_4}-L_4 & 0 & 0 & 0 \\ 0 & 0 & 0 & 0 & L_5 & 0 & 0 \\ 0 & 0 & 0 & 0 & 0 & X_{N_6}-L_6 & Y_{N_6}-L_7 \end{bmatrix} \begin{bmatrix} \dot{L}_1 \\ \dot{L}_2 \\ \dot{L}_3 \\ \dot{L}_4 \\ \dot{L}_5 \\ \dot{L}_6 \\ \dot{L}_7 \end{bmatrix}$$

3. SINGULARITY, DEXTERITY AND WORKSPACE ANALYSIS

3.1. Singularity Analysis

The forward and inverse kinematic singularity are the two categories of kinematic singularity. When the forward singularity of the manipulator occurs, the DOF of the input driving motion is lost, which means the input drive will exert invalidly in this direction. From a mathematical view, the forward singularity occurs when the rank of J_θ reduces. According to the geometric analysis, the lack of DOFs in certain directions will lead to the limited mobility of the mechanism. In this paper, when the forward singularity of the manipulator occurs, Eq.(26) must be satisfied.

$$det\left(\begin{bmatrix} Z_{N_1}-L_1 & 0 & 0 & 0 & 0 \\ 0 & Z_{N_2}-L_2 & 0 & 0 & 0 \\ 0 & 0 & L_3 & 0 & 0 \\ 0 & 0 & 0 & Z_{N_6}-L_4 & 0 \\ 0 & 0 & 0 & 0 & L_5 \end{bmatrix}\right) = 0 \quad (26)$$

From the above kinematic analysis, it can be seen that if one or more $\overrightarrow{\mathbf{U}_i\mathbf{N}_i}$ vectors are parallel to the *xy* plane of the fixed coordinate system, Eq.(26) will be satisfied. However, in practical design, S joint is always kept apart from the ground.

$$\begin{cases} L_6 - X_{N_6} = 0 \\ L_7 - Y_{N_7} = 0 \end{cases} \quad (27)$$

If the Eq.(27) is satisfied, the $\overrightarrow{\mathbf{U}_6\mathbf{N}_6}$ chain will became perpendicular to the *xy* plane, the manipulator will lose DOF in z-axis. The inverse singularity refers to the case that $J_a\dot{V} = J_\theta\dot{\theta}$ cannot be expressed as $\dot{V} = J\dot{\theta}$, i.e., $\mathrm{rank}(J_a) < 0$. The inverse singularity also means $J_a\dot{V} = 0$, i.e., in some certain directions any driving input will only result in zero instantaneous momentum, which will make the manipulator uncontrollable. Actually, if all the chains and the moving platform are in the same plane, an instantaneous DOF along z-axis will appear. However, the inverse singularity can be avoided by appropriate design of kinematic chain length. Another singularity configuration is that all the extension lines of the periphery chains and the central chain meet at one point. When it occurs, the mechanism can still work normally as the driving modes of the five periphery chains are different.

3.2. Dexterity Analysis

Dexterity is an important index for evaluating the manipulator performance. It is explicated as the kinematic ability of manipulator in specified direction at particular pose [11]. Here, the dexterity of the Jacobian matrix is used to evaluate the parallel manipulator's dexterity. And, the dexterity of the Jacobian matrix can be Figured out by

$$\kappa(J) = \frac{\sigma_{\min}(J)}{\sigma_{\max}(J)} \tag{28}$$

where $\kappa(\cdot)$ denotes the inverse condition number function, $\sigma_{\max}(J)$ and $\sigma_{\min}(J)$ are the maximum and minimum singular values of the Jacobian matrix J ,respectively.

In velocity Jacobian matrix, the output motion vector of the parallel manipulator proposed here are divided into two parts with different physical meanings, i.e, the linear velocity and the angular velocity. The dexterity for the linear velocity component of Jacobian matrix reflects the performance of linear velocity, while the one for angular velocity reflects the performance of angular velocity. Thus, they have different dimensions. Now, let us rewrite the Eq.(25) by

$$\begin{bmatrix} v \\ \omega \end{bmatrix} = \begin{bmatrix} J_v \\ J_w \end{bmatrix} \dot{L}_i \tag{29}$$

$\kappa(J_v)$ and $\kappa(J_w)$,respectively, are used to measure the position and orientation dexterities.

To guarantee the position and orientation dexterities over a chosen workspace, one can constrain the dexterity in the following form:

$$\kappa(J_v) \geq \kappa_1 \tag{30}$$

$$\kappa(J_w) \geq \kappa_2 \tag{31}$$

where κ_1 and κ_2 are the two thresholds for the position and orientation dexterities, which are constants assigned according to practical design requirements.

To show the distribution of the dexterities in the workspace, we give a numerical sampling as shown in Figure **3**, the computed square area is also given in Figure **3**. One can see that the manipulator has good dexterity in the sampling area of the workspace at different position when $(R, r, a, b, c) = (1.5, 0.5, 2, 0.5, 2)$, whose units are in mm.

3.3. Workspace Analysis

Workspace is a critical index to evaluate the performance of the parallel robot. In this paper, the numerical method based on searching method is used to obtain the boundary of the workspace.

In order to compute the numerical solutions of the feasible workspace, the initial design parameters of mechanism are set as $(R, a, b, r, c) = (1.5, 2, 0.5, 0.5, 2)$ with with units in mm. To compute the feasible workspace area, we must first discretize the pose coordinates of $(x, y, z, \phi, \theta, \psi)$, then verify the necessary kinematic constraints in every direction of the pose workspace. To determine the feasible workspace of the manipulator, the following constraints should be considered.

3.1. Real Solution

Verify whether each driver chain has real solution at designated pose $(x, y, z, \phi, \theta, \psi)$. The expression is written as follows:

$$isreal(L_i) = 1, \quad i = 1, 2, 3, 4, 5, 6, 7 \tag{32}$$

3.3.2. Range Restriction of Kinematic Pair

Kinematic pair's stroke is always limited in practical operation. One has to pay special attention to the joint limit of the five universal joints of the peripheral limbs and the two universal joints used in the centre limb, which is not explicitly shown in the inverse position kinematics equation. For the active joint variables, their limitations can be given as follows:

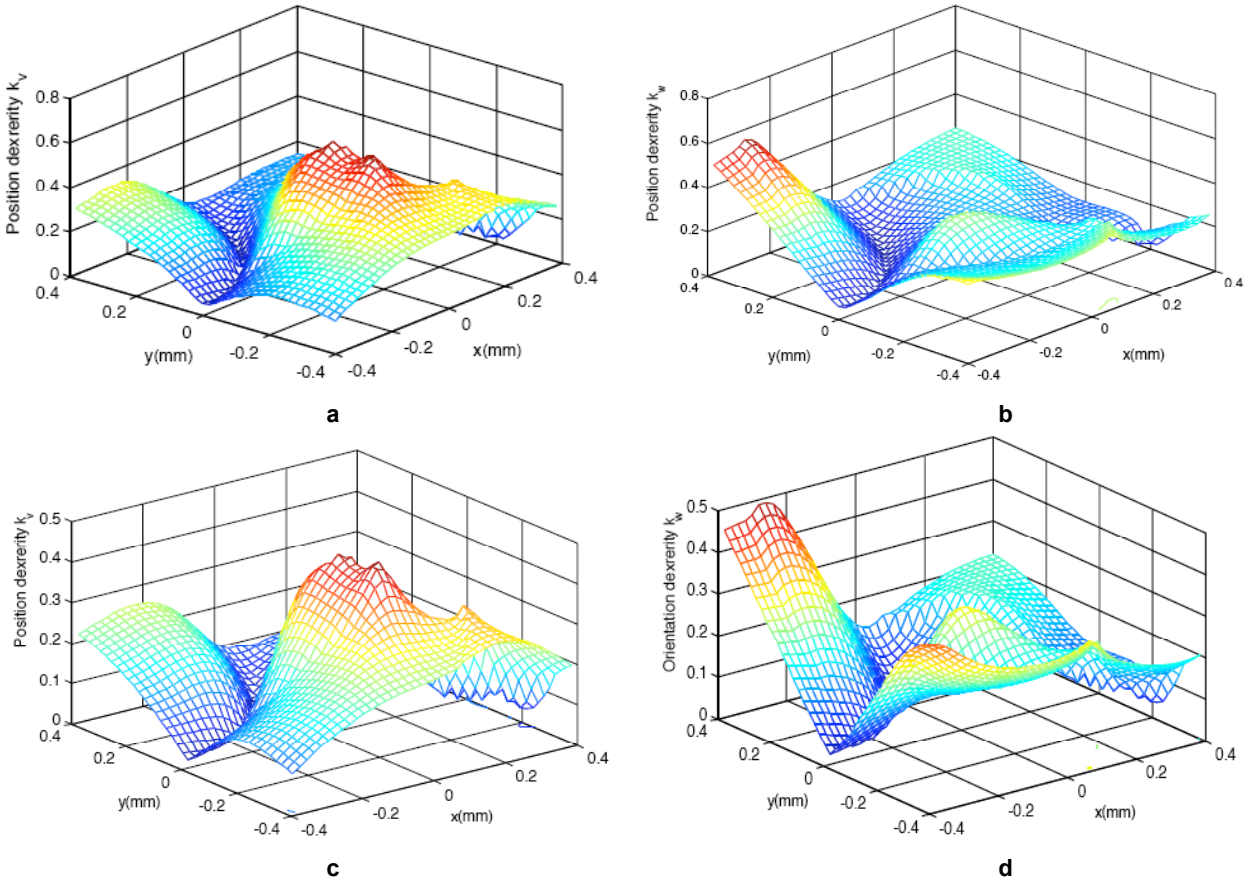

Figure 3: Dexterity distribution of the Jacobian matrix in the workspace at $x \in [-0.4, 0.4], y \in [-0.4, 0.4]$.(a) Maximum position dexterity $\kappa_{v\max}$ at z=2,(b) Maximum orientation dexterity $\kappa_{w\max}$ at z=2,(c) Maximum position dexterity $\kappa_{v\max}$ at z=2.2,(d) Maximum orientation dexterity $\kappa_{w\max}$ at z=2.2.

$$\begin{cases} -1 \le L_i \le 2, & (i = 1,2,4) \\ 1 \le L_i \le 4, & (i = 3,5) \\ -R\cos\dfrac{\pi}{5} \le L_i \le R\cos\dfrac{\pi}{5}, & (i = 6,7) \end{cases} \tag{33}$$

3.3.3. Constraint Conditions of Singularity

When it is found that the singular point is approaching, the constraint conditions of the position and orientation dexterities and the Jacobian matrix are needed to avoid singularity appearing. Table **1** need to be satisfied.

Table 1: Constraint Analysis of Singularity

Constraint conditions	Singularity Range
$\det(J_\theta^{'})$	$\left\|\det(J_\theta^{'})\right\| \ge 0.1$
$\sigma_{\min}(J_\theta)$	$\sigma_{\min}(J_\theta) \ge 0.1$
$\sigma_{\min}(J_a)$	$\sigma_{\min}(J_a) \ge 0.1$
The dexterities of J	$\kappa_{\min}(J_v) \ge 0.1, \kappa_{\min}(J_\omega) \ge 0.1$

3.3.4. Constraint Conditions of Tilting Angle

The tilting angle and rotating angle is one of the important criteria of manipulator. Based on different practical conditions, there are different requirements of them. In this paper, the manipulator's tilting angle and rotating angle both should be set no larger than $60°$.

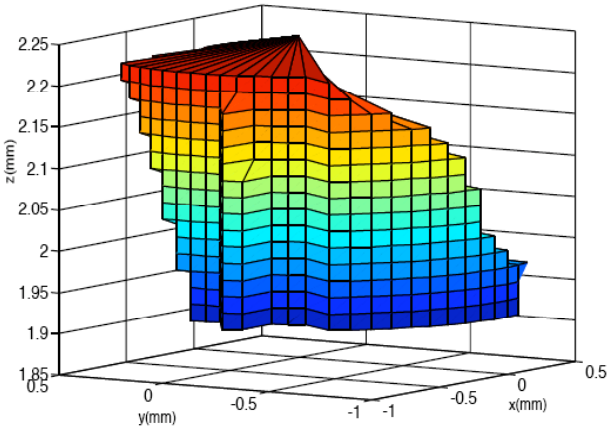

Figure 4: Workspace of the manipulator.

Using the four constraints given above, the 3D shape of usable workspace can be drawn as shown in Figure **4**.

4. CONCLUSION

A 6 DOFs adaptive parallel manipulator has been presented in this paper. Due to the special architecture, the doubly actuated centre limb of the manipulator has infinite inverse solutions in a circle. The analysis shows that the dexterity of the manipulator is different in different configurations of the centre limb. Thus, we can select the congratulation with best dexterity as the inverse solution of the centre limb. An optimization model for obtaining the optimized dexterity of the manipulator is introduced to solve this problem, which also makes the manipulator have large workspace because some singular congratulations can be eliminated by the adaptive motion of the centre limb. For further study, the position problems, singularity and workspace have also been studied, showing that the proposed manipulator has good dexterity and large workspace and it is a suitable candidate for some complicated surface machining.

ACKNOWLEDGEMENTS

This work is financially supported by the Natural Science Foundation of China (Grant No.: 51175105). The work is also supported by Shenzhen Research Grants (No. ZDSY20120613125132810, No. JCYJ20140417172417129).

REFERENCES

[1] Hailin Huang, Bing Li, Zongquan Deng, Ying Hu. A 6-DOF Adaptive Parallel Manipulator with Large Tilting Capacity. Robotics and Computer-Integrated Manufacturing 2012; 28(2): 275-283. http://dx.doi.org/10.1016/j.rcim.2011.09.009

[2] Stewart D. A Platform with Six Degrees of Freedom [C]. Proceedings Institute of Mechanism Engneering. London, England 1965; 180: 371-386.

[3] HRosario Sinatra H. A Different Kinematic Model of the Tricept Robot [C]. ASME Conference Proceedings 2002; 5: 1121-1128.

[4] Huang Z, Xia P. The Mobility Analyses of Some Classical Mechanism and Recent Parallel Robots [C]. ASME Conference Proceedings 2006; 2: 977-983.

[5] Innocenti C, Castelli VP. Forward Kinematics of the General 6-6 Fully Parallel Mechanism: an Exhaustive Numerical Approach *via* a Mono-Dimensional-Search Algorithm [J]. Journal of Mechanical Design 1993; 115(4): 932-937. http://dx.doi.org/10.1115/1.2919289

[6] Huang Z. Modeling Formulation of 6-DOF Multi-loop Parallel Manipulators. Part-2: Dynamic Modeling and Example [C]. Proc of the 4th IF To MM International Symposium on Linkage and Computer Aided Design Methods Bucharest. Romania 1985; 3(11): 163-170.

[7] Innocenti C, Castelli VP. Direct Position Analysis of the Steward Platform Mechanism [J]. Mechanism and Machine Theory 1990; 25(6): 611-621. http://dx.doi.org/10.1016/0094-114X(90)90004-4

[8] Wen FA, Liang CG. Displacement Analysis of the 6-6 Steward Platform Mechanisms [M]. Mechanism and Machine Theory 1994; 29(4): 547-557. http://dx.doi.org/10.1016/0094-114X(94)90094-9

[9] Innocenti C, Castelli VP. Closed-Form Direct Position Analysis of a 5-5 Parallel Mechanism [J]. Journal of Mechanical Design 1993; 115(3): 515-521. http://dx.doi.org/10.1115/1.2919220

[10] Stock M, Miller K. Optimal Kinematic Design of Spatial Parallel Manipulators: Application of Linear Delta Robot [J]. Journal of Mechanical Design 2003; 125(2): 292-301. http://dx.doi.org/10.1115/1.1563632

[11] Li B, Zhao J, Yang X, Hu Y. Kinematic Analysis of a Novel Three Degree-of-freedom Planar Parallel Manipulator. International Journal of Robotics and Automation 2009; 24(2): 158-165. http://dx.doi.org/10.2316/Journal.206.2009.2.206-3314

Received on 13-10-2014 Accepted on 31-10-2014 Published on 09-01-2015

DOI: http://dx.doi.org/10.15377/2409-9694.2014.01.02.1